JOURNAL OF CHEMICAL & ENGINEERING DATA

ARTICLE

pubs.acs.org/jced

Adsorption of Nickel Ions from Aqueous Solutions by Nano Alumina: Kinetic, Mass Transfer, and Equilibrium Studies

Varsha Srivastava,[†] C. H. Weng,[‡] V. K. Singh,[§] and Y. C. Sharma*[,†]

[†]Department of Applied Chemistry, and [‡]Department of Ceramic Engineering Institute of Technology, Banaras Hindu University, Varanasi 221 005, India

[§]Department of Civil and Ecological Engineering I-Shou University, Da-Hsu Hsiang, Kaohsiung County 84008, Taiwan

ABSTRACT: The presence of nickel in aquatic systems due to discharge of industrial effluents is of concern because of its toxic and nonbiodegradable nature. Its removal from water and wastewater is mandatory. Though activated carbon has been effective in removing metallic species including nickel from water and effluents, its high cost limits its large scale application to developing nations. The present paper addresses the removal of nickel from aqueous solutions by alumina nano particles. The adsorbent, nano alumina powder, was synthesized in the laboratory and was characterized by X-ray diffractometry (XRD), Fourier transformation infrared spectroscopy (FTIR), and transmission electron microscopy (TEM). The BET surface area and porosity of nanosized alumina powder were found to be 78.79 $m^2\ g^{-1}$ and 0.51, respectively. The initial concentration of nickel, agitation speed, and contact time were found to affect the removal of nickel from aqueous solutions. Kinetic studies were performed and pseudofirst order, second order, intraparticle diffusion, and mass transfer studies were carried out. The equilibrium data were analyzed by various isotherms viz. Langmuir, Freundlich, Dubinin−Radushkevich, and Temkin and Pyzhev isotherms. Results of the present study revealed that nano particles of alumina powder can be used for a large scale treatment of water containing Ni(II) in particular and that of pollutant species in general.

1. INTRODUCTION

The presence of heavy metals in the environment is of major concern because of their toxicity and tendency for bioaccumulation in the food chain even at relatively low concentrations. Because of their toxicity and various harmful effects, most of the heavy metals have been recognized as priority pollutants and have been reported to accumulate in the environment causing potential short-term and long-term adverse effects to fauna, flora, and humans.[1,2] The tremendous increase in the use of heavy metals in different industrial applications, especially over the past few decades, has inevitably resulted in an increased amount of "metal pollution" of water bodies. Nickel is regularly used in the manufacture of stainless steel, coins, metallic alloys, super alloys, nonferrous metals, mineral processing, paint formulation, electroplating, batteries manufacturing, forging, porcelain enameling, copper sulfate manufacture, and steam-electric power plants.[3−5] Nickel may be beneficial as an activator of some enzyme systems in trace amounts and is identified as participating in important metabolic reactions; its intake in higher concentrations results in different types of diseases such as pulmonary fibrosis, lung cancer, renal edema, and skin dermatitis. Some nickel compounds such as the carbonyls are carcinogenic and are easily absorbed by skin.[6]

In view of the toxicity, wastewaters rich in nickel should be properly treated prior to their discharge. Conventional methods for removal of nickel from aqueous solutions include solvent extraction, electrochemical treatment, ion exchange, chemical precipitation, chemical oxidation/reduction, filtration, reverse osmosis, membrane technologies and evaporation recovery.[7−11] Most of the methods have their inherent merits and demerits. Some of them are extremely expensive. A major disadvantage with conventional treatment methods is the production of toxic chemical sludge. The disposal/treatment of the sludge is expensive and "non eco-friendly". Comparatively, the adsorption process seems to be a more attractive method in water pollution control in terms of cost, simplicity of design, and operation.[12] Activated carbon is a promising and widely used adsorbent for wastewater treatment and has been successfully used for the removal of various types of pollutants including metallic species. However, because of high cost, its large scale application is limited to developed nations only. A variety of waste materials, minerals, and clays have also been used as adsorbents for the removal of a variety of pollutants at the laboratory scale, but they offer a very low efficiency of removal. Nanosized materials are new functional materials, which offer high surface area and have come up as effective adsorbents.[13] Nano alumina is one of the most important ceramic materials widely used as an electrical insulator, presenting exceptionally high resistance to chemical agents, as well as giving excellent performance as a catalyst for many chemical reactions, in microelectronic, membrane applications, and water and wastewater treatment.[14,15] Pure alumina nanoparticles have been synthesized by a variety of techniques such as controlled precipitation, ultrasonic flame pyrolysis, gel combustion, sol−gel, and the combustion method.[16] Among

Special Issue: John M. Prausnitz Festschrift

Received: October 30, 2010
Accepted: March 11, 2011
Published: March 25, 2011

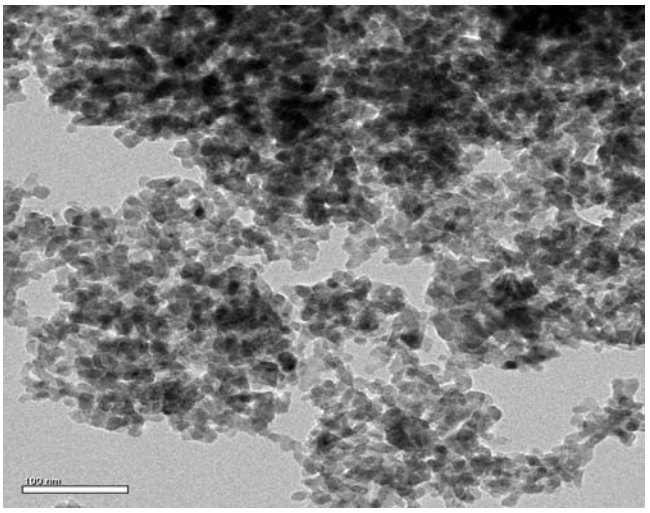

Figure 1. TEM of nanoadsorbent alumina powder.

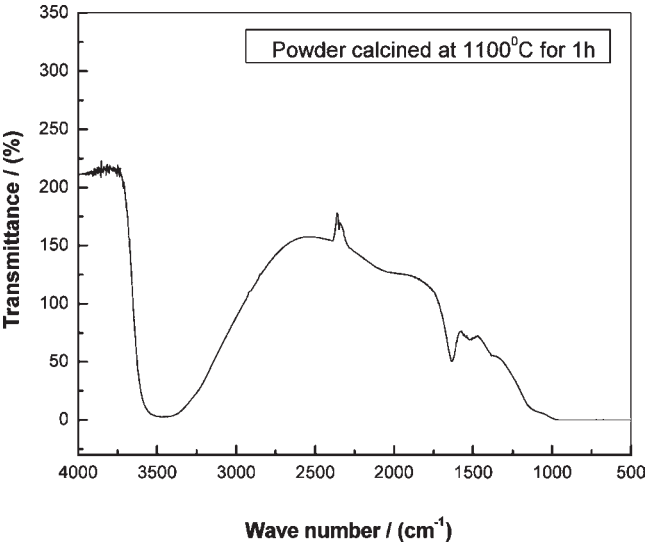

Figure 2. FTIR of nanoadsorbent alumina powder.

various available methods, the sol−gel method is simple and cost-effective for the synthesis of nanosized alumina. By the sol−gel method, the size and morphology of nanoparticles can also be controlled.

In the present study, nano alumina was synthesized by the sol−gel method and used for the adsorption of nickel ions from their aqueous solutions. For the adsorption of Ni(II) from aqueous solutions, batch adsorption experiments were conducted and various important parameters affecting the removal process were optimized. Kinetics and equilibrium studies were carried out for a better understanding of adsorption process.

2. EXPERIMENTAL SECTION

All the chemicals used in the present study were of AR/GR grade and were procured from Merck, Mumbai, India. Nano alumina powder was synthesized by using the sol−gel method. The details of synthesis of the nano alumina powder are reported elsewhere.[10] The adsorbent nano alumina was characterized by different techniques viz. XRD, TEM and FTIR. The BET surface area of alumina adsorbent was also determined.

2.1. Determination of pH_{zpc} (Point of Zero Charge). pH_{zpc} is a fundamental property of a water/oxide interface. Determination of pH_{zpc} was done to investigate the surface behavior of nano alumina powder.[17,18] For determination of pH_{zpc}, a solution of 0.01 M NaCl was prepared, and its pH was adjusted in the range between 2 and 12 by using NaOH or HCl. Then 50 mL of 0.01 M NaCl was taken in a flask and 0.20 g of the adsorbent was added in flasks containing 0.01 M NaCl solution of different pH values. These flasks were then kept for 48 h and after that the pH of the solutions was measured by using a pH meter (IKON digital pH meter). A graph was then plotted between pH_{final} vs $pH_{initial}$. The point of intersection of the "pH_{final} vs $pH_{initial}$" curves represents the pH_{zpc} of the adsorbent.

2.2. Adsorption Experiments. The adsorbent, nano alumina powder was used for the removal of Ni(II) from aqueous solutions and the effect of various important parameters on removal of Ni(II) was studied. For the removal of Ni(II), usual batch adsorption experiments were conducted. A stock solution of Ni(II) was prepared by dissolving nickel sulfate in 1000 mL of distilled water and this solution was used to prepare working solutions of Ni(II) of different concentrations. The ionic strength of the aqueous solutions was maintained at 1.0 × 10^{-2} M $NaClO_4$. For batch adsorption experiments, 0.25 g of adsorbent was added to 50 mL of aqueous solutions of Ni(II) ions of varying concentration in 250 mL stoppered conical flasks. All of the adsorption experiments were conducted at (25 ± 0.5) °C, at a pH of the working solution and agitation rate of 100 rpm on a shaking thermostat. After the equilibrium time, the adsorbent was separated from the aqueous phase by centrifugation at 10 000 rpm for 10 min.

The amount of metallic ions adsorbed per unit mass of the adsorbent was determined by using the following equation:

$$q_e = (C_i - C_e/W)V \quad (1)$$

where q_e is the amount adsorbed per unit mass of the adsorbent ($mg \cdot g^{-1}$), C_i and C_e are the initial and equilibrium concentrations of the adsorbate, respectively ($mg\ L^{-1}$), W is the mass of adsorbent (g), and V (L) is volume of the solution.

The percentage removal of metallic ions was calculated from the following equation:

$$\%\ \text{removal of metallic ions} = (C_i - C_e/C_i) \times 100 \quad (2)$$

The residual concentration of Ni(II) in the supernatants were determined by a UV−visible spectrophotometer (Spectronic 20, Bausch and Lomb; USA) at 445 nm with a dimethyl glyoxime (DMG) method by following the standard methods.[19]

3. RESULTS AND DISCUSSION

3.1. Characterization of the Adsorbent. Nanoalumina powder was characterized by XRD for its phase confirmation and determination of the diameter of the particles (figure not given). A TEM of the adsorbent particles shows that the particles are of nano size (Figure 1).

Surface characteristics of the adsorbent particles were investigated by FTIR. FTIR spectra of the bare and Ni(II) loaded adsorbent are shown in Figures 2 and 3. In nano alumina, the vibrations of OH and Al−OH and Al−O bonds generated are observed in the infrared region. The stretching vibration of the OH^- ions of residual water and solvent in the gel produced are indicated by a very intense broad band at (3000 to 3600) cm^{-1}, whereas their bending vibration generated the band at 1632 cm^{-1}.[20]

dx.doi.org/10.1021/je101152b |J. Chem. Eng. Data 2011, 56, 1414–1422

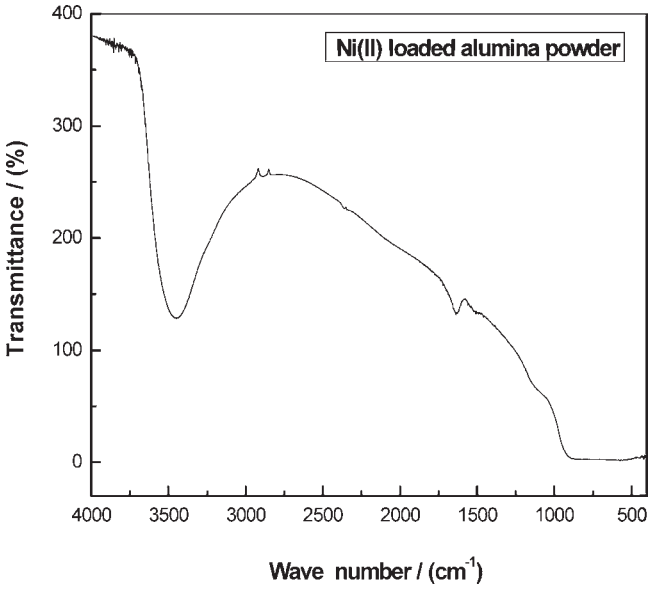

Figure 3. FTIR of Ni(II) loaded nanoadsorbent alumina powder.

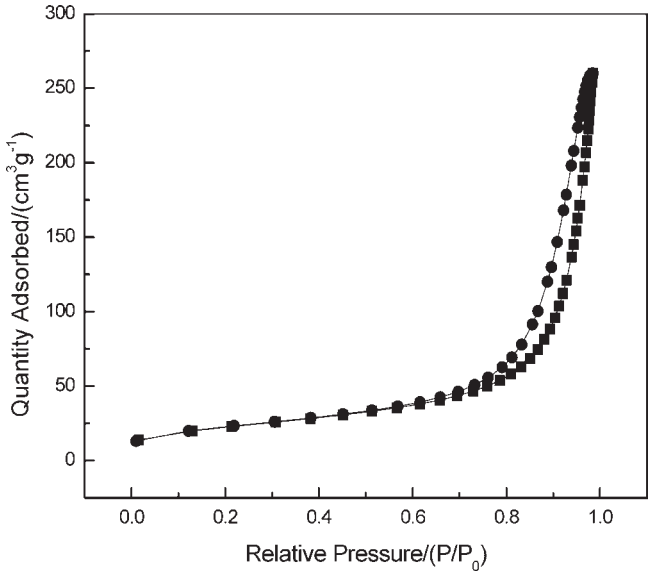

Figure 4. N_2 gas adsorption -desorption isotherm for the nanoadsorbent alumina powder (■, adsorption; ●, desorption).

The presence of peaks in the region (3000 to 3600) cm^{-1} is related to the lattice of water molecules. They indicate the presence of moisture in the powder or KBr. The stretching vibrations of the Al−OH bond gave rise to the band at 1555 cm^{-1}. The weak bands observed between (1100 to 1200) cm^{-1} were produced by the Al−O bonds.[21]

There is no significant change in the FTIR of bare and Ni(II) loaded nano adsorbent alumina powder (Figures 2 and 3) which confirms that there is no formation of new groups between the adsorbates and adsorbents. Plots of N_2 gas adsorption−desorption isotherms, for nanoadsorbent alumina powder, are shown in Figure 4. The surface area of the nanoadsorbent was found to be 78.798 $m^2 \cdot g^{-1}$.

The pH_{zpc} of nanoadsorbent alumina powder was determined from the point of intersection of the $pH_{initial}$ vs pH_{final} curve with

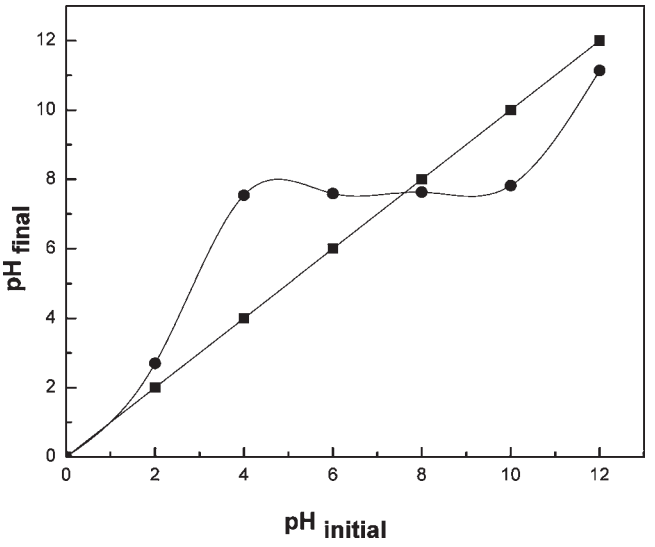

Figure 5. Plot for determination of pH_{zpc} of nanoadsorbent alumina powder (■, $pH_{initial}$ vs pH_{final}(without adsorbent); ●, $pH_{initial}$ vs pH_{final} (with adsorbent).

Table 1. Characterization of Nanoadsorbent Alumina Powder

characterization of nanoadsorbent alumina	
phase	γ and α-Al_2O_3
particle diameter/(nm)	15−20
BET surface area/($m^2 \cdot g^{-1}$)	78.79
porosity	0.51
density/($g \cdot cm^{-3}$)	1.33
pH_{zpc}	7.9

the $pH_{initial}$− pH_{final} line (Figure 5) and was found to be 7.9. In the literature, it is reported that alumina has a hydroxylated surface and it has $pH_{zpc} \approx 9.2$ but as alumina is calcined above 1000 °C, its pH_{zpc} decreases.[22] Similar observations have been observed in the present study also.

3.2. Determination of Time of Equilibrium and Optimum Ni(II) Concentration. A study of the effect of contact time and concentration on adsorption of Ni(II) on nanoadsorbent alumina shows that removal increased from (96.60 to 99.0) % by decreasing the concentration of Ni(II) in solution from (75 to 25) $mg \cdot L^{-1}$ at 25 °C and 0.01 M $NaClO_4$ ionic strength (Figure 6). The equilibrium time was found to be 120 min. These findings reveal that the adsorption process is highly dependent on the initial concentration of Ni(II) ions. A higher removal at lower concentration is of industrial importance.

3.3. Determination of Optimum Agitation Speed. Adsorption of metallic ions from aqueous solutions is influenced by agitation speed also. Knowledge of agitation speed is important because agitation speed influences the distribution of the solute in the bulk solution.[23,24] Agitation rate is an important parameter, since it can promote a certain turbulence which ensures an intimate contact between the two phases (adsorbent−adsorbate). In present study three different agitation speeds (50, 75, and 100) rpm were selected to investigate the effect of agitation speed on the removal of metallic species by adsorption on the selected adsorbent. During this study, all other parameters were

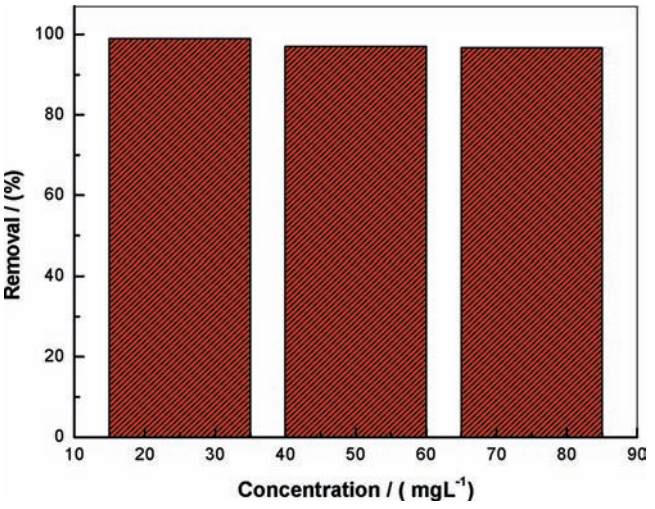

Figure 6. Effect of initial concentration and contact time on the removal of Ni(II) by adsorption on nanoadsorbent alumina powder.

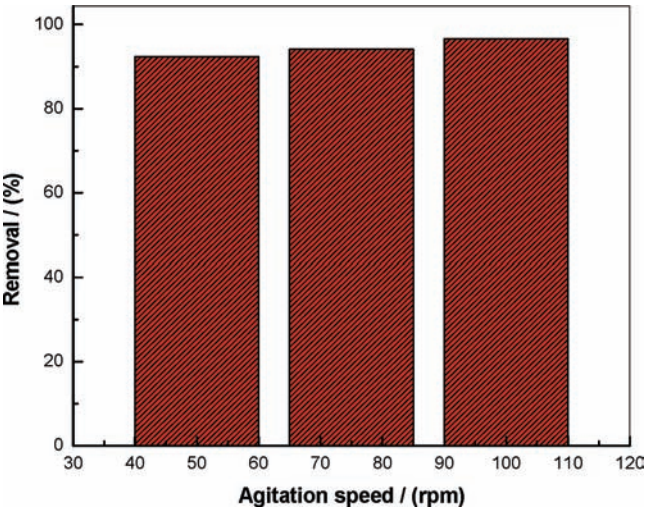

Figure 7. Effect of agitation speed on the removal of Ni(II) by adsorption on nanoadsorbent alumina powder.

kept constant. It is clear from Figure 7 that removal of metallic ions increases by increasing agitation speed. It was found to be a maximum (96.6 %) at the highest agitation speed (Figure 7). An increasing trend of removal by increasing agitation speed was also reported earlier.[25] The results indicate that a moderate speed of 100 rpm was optimum as it facilitates proper contact between the metal ions in solution and the binding sites and thereby promotes effective transfer of adsorbate ions to the adsorbent surface and the sites. Further, for the study of the effect of "mixing rate" on removal (%) of Ni(II) by adsorption, it was found that at 100 rpm removal was higher. After optimizing the value of the mixing rate, this value has been used for the study of other parameters. Experiments were conducted at 150 rpm also, but the change in removal at this rpm was not significant, and because of this, a rpm of 100 was taken as optimum in the experiments.

4. KINETIC MODELING FOR THE REMOVAL OF NI(II) FROM AQUEOUS SOLUTIONS

4.1. Pseudofirst Order Kinetic Model. The pseudofirst order model can be expressed by following the equation:[26]

$$\frac{dq}{dt} = k_1(q_e - q_t) \tag{3}$$

The integrated form of the above expression is as follows:

$$\log(q_e - q) = \log q_e - \frac{k_1}{2.303}\, t \tag{4}$$

k_1 (min^{-1}) is the first order rate constant, q_e and q are the amounts of adsorbate species adsorbed at equilibrium and at any time respectively ($mg\ g^{-1}$). The value of k_1 was determined from the slope of the linear plots of $\log(q_e - q)$ vs t at different temperatures (figure not given).

4.2. Pseudo-second Order Kinetic Model. The kinetic data were also analyzed by the pseudo second order kinetic equation. The second order model assumes that the rate limiting step is chemisorption in nature. The mechanism may involve valence forces by sharing or through the exchange of electrons between adsorbent and adsorbate. This can be expressed as follows:[27]

$$\frac{dq}{dt} = k_2(q_e - q_t)^2 \tag{5}$$

Table 2. Pseudo-First Order and Pseudo-Second Order Rate Constants for the Removal of Ni(II) by Adsorption on Nano Alumina at Different Temperatures

	pseudo-second order model			
temperature	k_1		k_1	
± 0.5 °C	$\times 10^{-2}$ min^{-1}	R^2	$\times 10^{-2}$ min^{-1}	R^2
25	1.83	0.979	0.266	0.999
35	1.95	0.991	0.261	1
45	2.30	0.996	0.683	1

where k_2 ($g \cdot mg^{-1} \cdot min^{-1}$) is the rate constant of the pseudo-second order kinetic equation. The integrated form of above equation can be expressed as follows:

$$\frac{t}{q_t} = \frac{1}{k_2 {q_e}^2} + \frac{1}{q_t}\, t \tag{6}$$

$$h = k_2 {q_e}^2 \tag{7}$$

h is known as the initial sorption rate. The value of q_e and k_2 can be determined by the slope and intercepts of the straight line of the plot "(t/q_t vs t)", respectively (figure not given). The values of the pseudofirst order and pseudosecond order rate constants for the removal of Ni(II) by adsorption on nano alumina at different temperatures are given in Table 2. It is clear from Table 2 that values of k_1 increase by increasing temperature which confirms the endothermic nature of Ni(II) adsorption on nano alumina. Experimental values of q_e did not agree with the calculated values obtained from the linear plots of the pseudo-first order equation. Values of calculated q_e from the pseudo-second order kinetics almost agreed with the experimental values of q_e.

4.3. Intraparticle Diffusion Study. The most commonly used technique for identifying the mechanism involved in the sorption process is by fitting the experimental data to an intraparticle diffusion model. The overall adsorption of solute onto the solid surface may be controlled by one or more steps, e.g., boundary

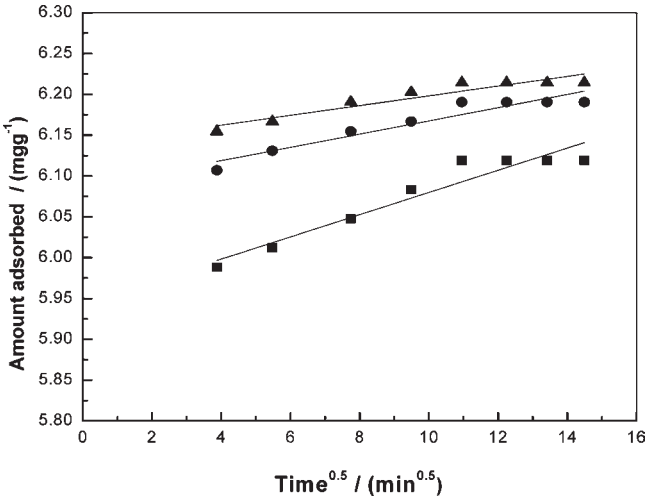

Figure 8. Intraparticle diffusion plots for the removal of Ni(II) by adsorption on nanoadsorbent alumina powder at different temperatures. (■) (25 ± 0.5) °C; (●) (35 ± 0.5) °C; and (▲) (45 ± 0.5) °C.

Table 3. Intraparticle Diffusion Rate Constant for the Removal of Ni(II) by Adsorption on Nanoadsorbent Alumina Powder at Different Temperatures

	intraparticle diffusion rate constant
temperature	K_{id}
±0.5 °C	$\times 10^{-2}$ mg·g^{-1}·min^{-1}
25	1.36
35	0.08
45	0.06

layer (film) or external diffusion, pore diffusion, surface diffusion and adsorption onto the pore surface or in combination of several steps.

Generally, an adsorption process is diffusion controlled, if the rate is dependent on the rate of diffusion of the components toward one another. Previous studies have reported that the plot of q_t vs $t^{1/2}$ represents multilinearity, which characterizes the two or more steps that are involved in the sorption process. In usual batch experiments also, the adsorption can occur by intraparticle diffusion. To confirm this, values of the rate constant of intraparticle diffusion k_{id} were calculated from the slopes of the linear portions of the plots of "amount adsorbed vs square root of time" (Figure 8) at different temperatures by using the following equation:[28]

$$q_t = k_{id} t^{1/2} \tag{8}$$

where q_t is the amount adsorbed at time t (mg·g^{-1}), and $t^{1/2}$ is the square root of the time (min$^{1/2}$). It is an empirically found functional relationship common to most adsorption processes where uptake varies almost proportionally with $t^{1/2}$ rather than with contact time. The values of k_{id} were calculated from the slope of curves at different temperatures from intraparticle diffusion plots (Figure 8) and are given in Table 3. Diffusion is an endothermic process and the rate of adsorption will increase with an increased solution temperature when pore diffusion is the rate limiting step.[29] In the present study, the process is expected to be controlled by pore diffusion. The sorption at higher temperatures becomes more dependent on intraparticle

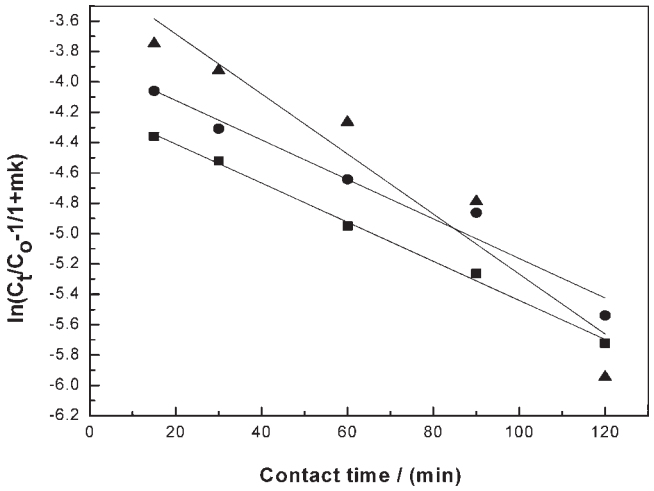

Figure 9. Mass transfer plots for the removal of Ni(II) by adsorption on nanoadsorbent alumina powder at different temperatures. (■) (25 ± 0.5) °C; (●) (35 ± 0.5) °C; and (▲) (45 ± 0.5) °C.

diffusion, which would be the rate limiting step.[30] Slope of final linear portion is a measure of intraparticle pore diffusion.[28]

4.4. Mass Transfer Study. For any process of removal by adsorption, it is important to know the extent of transfer of a pollutant species from the bulk to the surface of the solid adsorbent particles and at the interface of liquid and solid particles. A number of steps can be considered participating in the process of removal and the overall removal by sorption is assumed to occur using a three step model:[31]

i. Mass transfer of solute from the aqueous phase onto the solid surface.
ii. Sorption of solute on to the surface sites.
iii. Internal diffusion of solute via either a pore diffusion model or homogeneous solid phase diffusion model.

During the present studies, step (ii) has been assumed rapid enough with respect to other steps and therefore is not the rate limiting step in these studies. For recent studies this probability was examined by using the following mass transfer model:[31]

$$\ln\left(\frac{C_t}{C_0} - \frac{1}{(1+mk)}\right) = \ln\left(\frac{mk}{1+mk}\right) - \left(\frac{1+mk}{mk}\right)\beta_L S_s t \tag{9}$$

where k is a constant and is the product of Langmuir's parameters, m is the mass of the adsorbent per unit volume, β_L (cm·s^{-1}), the coefficient of mass transfer, S_s is the specific surface area. The values of m and S_s have been determined as follows:

$$m = \frac{W}{V} \tag{10}$$

$$S_s = \frac{6m}{d_p \delta_p (1-\varepsilon_p)} \tag{11}$$

where ε_p is the porosity of the adsorbent, d_p is the diameter of the adsorbent, and δ_p is the density of adsorbent.

Values of β_L, the coefficient of mass transfer, were calculated at different temperatures by the slopes and intercepts of the plots of $\ln[(C_t/C_0) - 1/(1 + mk)]$ vs t (Figure 9) and are given in Table 4. A value of β_L of the order of 10^{-5} or greater shows that

dx.doi.org/10.1021/je101152b |J. Chem. Eng. Data 2011, 56, 1414–1422

Table 4. Values of the Mass Transfer Coefficient for the Removal of Ni(II) by Adsorption on Nanoadsorbent Alumina Powder at Different Temperatures

	coefficient of mass transfer
temperature	$\beta_L \times 10^{-5}$
± 0.5 °C	cm·s^{-1}
25	0.55
35	0.57
45	0.85

the rate of transfer of mass from the bulk to the solid surface is rapid enough.[32] It is clear from the perusal of the plots that some points deviate from linearity. This is because of the variation in the extent of mass transfer at those stages.

5. EFFECT OF TEMPERATURE OF NI(II) REMOVAL BY NANOADSORBENT ALUMINA POWDER

Temperature is an important parameter affecting adsorption processes. Most adsorption processes are exothermic in nature but in some cases, endothermic adsorption is also reported.[11] It is considered that in endothermic processes, the number of active sites on the adsorbent increase with increasing temperature. Due to availability of more number of active sites, adsorption of the species increases by increasing temperature. In the present investigations the adsorption of Ni(II) by nanoadsorbent alumina was investigated at (25, 35, and 45 (± 0.5)) °C. The other experimental conditions viz. pH, concentration, dose and agitation speed were constant. The ionic strength of the aqueous solutions was maintained at 1.0 × 10^{-2} M $NaClO_4$. The adsorption of Ni(II) ions has been found to increase with an increase in temperature from (25 to 45) °C. It may be attributed to either an increase in the number of active sites available or the desolvation of the adsorbing species and the decrease in the thickness of the boundary layer surrounding the adsorbent with the temperature, so that the mass transfer resistance of the adsorbate in the boundary layer decreases.[10]

6. DETERMINATION OF ACTIVATION ENERGY

Activation energy, E_a, can be calculated by using the Arrhenius equation:[33]

$$\ln k = \ln A - \frac{E_a}{RT} \tag{12}$$

where A is the frequency factor (min^{-1}), k = rate constant value for the metal adsorption, E_a = activation energy in kJ·mol^{-1}, T = temperature (K), and R = 8.314 kJ·mol^{-1}·K^{-1}.

The value of E_a can be calculated by the slope of graph ln k vs 1000/T (Figure 10). The activation energy was found to be 8.96 kJ·mol^{-1}. A low activation energy indicates that the removal of Ni by nano alumina occurs through physical adsorption.

7. ADSORPTION ISOTHERMS FOR THE REMOVAL OF NI(II) FROM AQUEOUS SOLUTIONS

Adsorption isotherms are important tools for the analysis of adsorption processes as they provide information on the initial experimental setup to determine the feasibility of an adsorption treatment. Eequilibrium studies are useful to obtain the adsorption

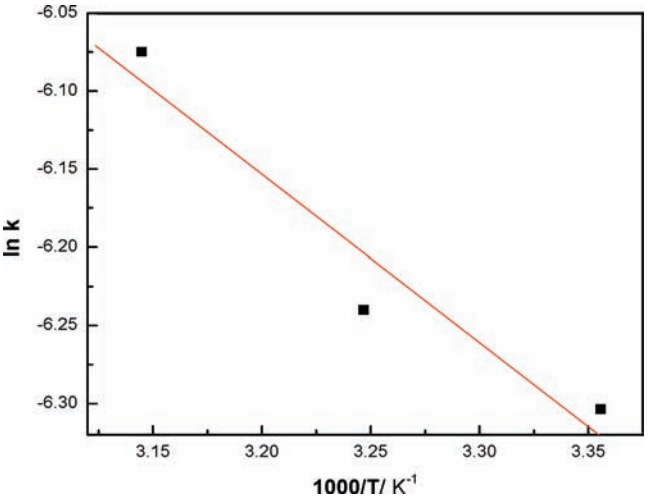

Figure 10. Plot of ln k vs 1000/T for determination of activation energy.

capacity of the adsorbents. To get the equilibrium data, initial concentrations were varied while the adsorbent dose in each sample was kept constant. The time of equilibrium was chosen considering the results of kinetic studies of metal removal by nano alumina. Equilibrium data were generated by mixing the nanoadsorbent in 50 mL of metal solution of desired concentration. After equilibrium, the nanoadsorbents were separated from the solution by centrifugation. The residual concentrations of metallic ions in the bulk were determined. Three different temperature viz. (25, 35, and 45 (± 0.5)) °C were selected for the equilibrium studies. The ionic strength of the aqueous solutions of metallic ions was maintained at 1.0 × 10^{-2} M $NaClO_4$. In the present study different isotherms such as the Langmuir, Freundlich, Dubinin−Radushkevich, and Temkin isotherms were used.[34−38]

7.1. Langmuir Adsorption Isotherm. The Langmuir adsorption isotherm model is valid for a mono layered coverage of adsorbent by the solute. The Langmuir isotherm is based on the assumption that maximum adsorption corresponds to a saturated monolayer of solute molecules on the adsorbent surface, that the energy of adsorption is constant. The linearized expression of the Langmuir model can be expressed as follows:[34]

$$\frac{C_e}{q_e} = \frac{1}{Q^0 b} + \frac{C_e}{Q^0} \tag{13}$$

where C_e (mg·L^{-1}) and q_e (mg·g^{-1}) are the concentrations of adsorbate and amount of adsorbate adsorbed at equilibrium, respectively. Q^0 (mg·g^{-1}) and b (L·mg^{-1}) are the terms related to capacity and energy of adsorption, respectively, and are known as Langmuir's constants. The equilibrium data were plotted as C_e/q_e vs C_e.

Langmuir capacities were calculated by using eq 13. The data has been plotted as C_e/q_e vs C_e (figure not given). The values of Q^0 and b were found to be 30.82 mg·g^{-1} and 0.49 L·mg^{-1} respectively at 298 K. For the Langmuir isotherm, a dimensionless separation factor can be expressed by the following equation:[35]

$$R_L = \frac{1}{(1 + bC_0)} \tag{14}$$

where C_0 is the initial solute concentration (mg·L^{-1}) and b is the Langmuir adsorption equilibrium constant (L·mg^{-1}). The dimensionless constant separation factor, R_L, is used to test

Table 5. Values of the Dimensionless Constant Separation Factor, R_L, for the Removal of Ni(II) by Adsorption at Different Temperatures

temperature ± 0.5 °C	R_L
25	0.0018
35	0.0017
45	0.0013

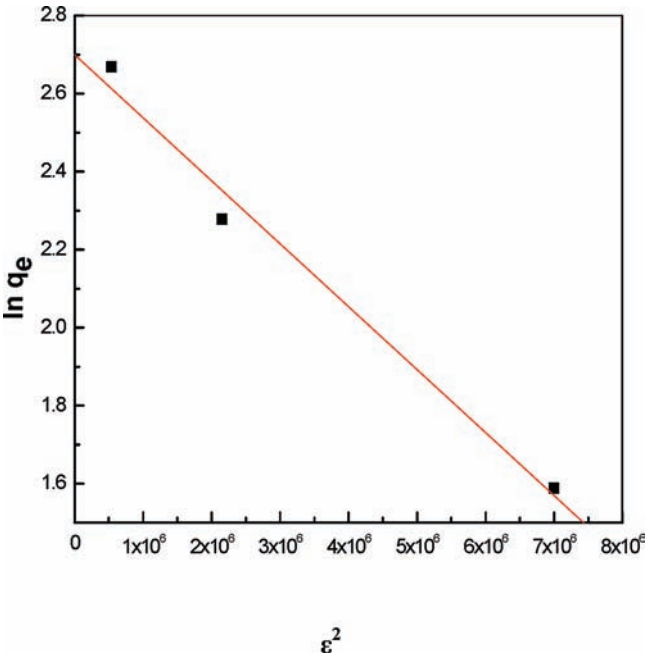

Figure 11. Dubinin−Radushkevich isotherm of Ni(II) on nanoadsorbent alumina.

whether the adsorption is favorable or not. The value of R_L indicates the type of the isotherm to be either unfavorable ($R_L > 1$), linear ($R_L = 1$), favorable ($0 < R_L < 1$), or irreversible ($R_L = 0$). The values of R_L are given in Table 5. The value of R_L further confirms the validity of this model. The values of R_L are $0 < R_L < 1$ and suggest that for adsorption of Ni(II) on nanoadsorbent alumina is favorable.

7.2. Freundlich Adsorption Isotherm. The equilibrium data were also examined by the Freundlich adsorption isotherm. The Freundlich model assumes that the uptake of metal ions occurs on a heterogeneous adsorbent surface. The Freundlich equation indicates the adsorptive capacity or loading factor on the adsorbent surface. The Freundlich model is expressed as follows:

$$q_e = K_f C^{1/n} \tag{15}$$

The logarithmic form of the equation is expressed as follows:[36]

$$\log q_e = \log K_f + 1/(n \log C_e) \tag{16}$$

where K_f is the Freundlich constant denoting adsorption capacity ($mg \cdot g^{-1}$) and $1/n$ is the empirical constant indicating adsorption intensity ($L \cdot mg^{-1}$) and depends on the temperature and

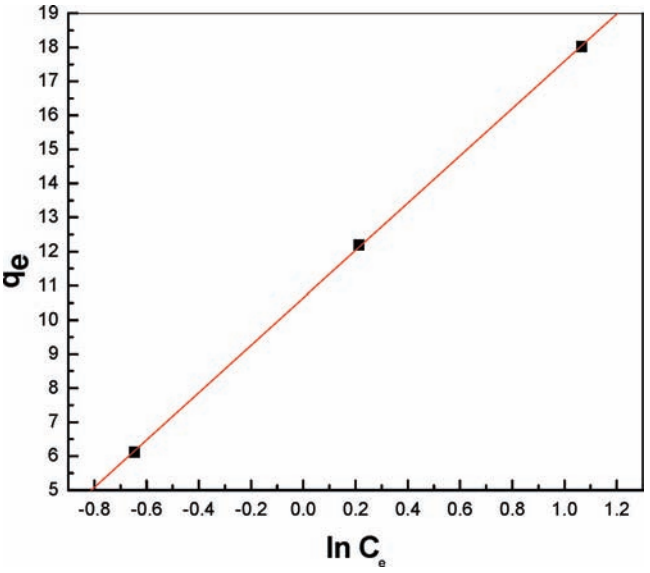

Figure 12. Temkin plot for adsorption of Ni(II) on nanoadsorbent alumina powder.

properties of the adsorbate and adsorbent. They are measure of adsorption capacity of the adsorbent and adsorption intensity respectively. C_e is the residual concentration of the solute remaining in the solution ($mg \cdot L^{-1}$), q_e is the amount of adsorbate adsorbed by a unit mass of adsorbent at equilibrium ($mg \cdot g^{-1}$). The value of K_f and n are calculated by the slopes and intercepts of the plots of log C_e vs log q_e. The values of K_f and n were found to be 9.66 $mg \cdot g^{-1}$ and 1.59 $L \cdot mg^{-1}$ at 298 K.

7.3. Dubinin−Radushkevich (D-R) Isotherm. To investigate the nature of the adsorption process, the D-R isotherm was applied for experimental data. The D-R isotherm does not assume a homogeneous surface or constant sorption potential. The D-R equation can be expressed as follows:[37]

$$q_e = q_m \exp(-B\varepsilon^2) \tag{17}$$

The linear form of above equation can be expressed as

$$\ln q_e = \ln q_m - B\varepsilon^2 \tag{18}$$

$$\varepsilon^2 = RT \ln\left(1 + \frac{1}{C_e}\right) \tag{19}$$

where R is the gas constant (8.314 $J \cdot mol^{-1} \cdot K^{-1}$) and T is the absolute temperature. The values of q_m and B can be obtained by the intercept and slope of the graph of ln q_e vs ε^2 (Figure 11).

The values of B and q_m were found to be 16.13×10^{-8} and 489.77 $mg \cdot g^{-1}$ respectively at 298 K

$$E = \left(\frac{1}{\sqrt{2B}}\right) \tag{20}$$

where E is the mean free energy of sorption per molecule of the sorbate ($kJ \cdot mol^{-1}$)

The magnitude of E determines the type of adsorption process. The value of E was found to be 17.60×10^{-5} $kJ \cdot mol^{-1}$ at 298 K.

7.4. Temkin and Pyzhev Isotherm. According to this isotherm the adsorption in the layer decreases by the coverage due

to interaction between adsorbate and adsorbent:[38]

$$q_e = \frac{RT}{b} \ln AC_e \quad (21)$$

$$q_e = B_1 \ln A + B_1 \ln C_e \quad (22)$$

where $B_1 = RT/b$, T = absolute temperature (K), R = gas constant (8.314 $J \cdot mol^{-1} \cdot K^{-1}$), A = equilibrium binding constant, q_e = amount of adsorbed Ni(II) per unit weight of adsorbent ($mg \cdot g^{-1}$), and C_e = concentration of Ni(II) ions in aqueous solution at equilibrium. The values of B_1 and A can be calculated by a slope and intercept respectively from a graph of q_e versus ln C_e (Figure 12). B_1 is related to the heat of adsorption. The values of B_1 and A were found to be 5.55 $mg \cdot g^{-1}$ and 35.73 $L \cdot mg^{-1}$ at 298 K.

It was also possible to test the equilibrium data using one isotherm equation only, but in order to ascertain validity of data over a wide range of considerations, the data were tested with the selected models. Interestingly, more than one model fitted the data satisfactorily. Further, at one tempearature, a particular model was more suitable and at other temperature, another model was more suitable.

8. CONCLUSIONS

On the basis of present studies the following conclusions may be drawn:

- Nano alumina was successfully synthesized by the sol−gel method and its size was found to be in (15 to 20) nm range. The surface area of nanoadsorbent alumina was 78.79 $m^2 \cdot g^{-1}$.
- FTIR of the bare and Ni(II) loaded nanoadsorbent confirmed that there is no change in surface characteristics of the nanoadsorbent after adsorption.
- The pH_{zpc} of nanoadsorbent alumina was determined and found to be 7.9.
- Initial concentration and contact time were found to affect the removal process and % removal of Ni was found to increase on decreasing the initial adsorbate concentration.
- Agitation speed also affects removal of adsorbates. Removal of Ni(II) ions was a maximum at 100 rpm.
- The removal process follows pseudo-second order kinetics better.
- The values of the coefficient of mass transfer for the systems were significant and are indicative of a sufficiently rapid transfer of adsorbate species from the bulk to the surface and/or solid/liquid interface.
- The activation energy was found to be 8.96 kJ mol^{-1}.
- The Langmuir, Freundlich, Dubinin−Radushkevich, and Temkin and Pyzhev isotherm studies further confirm the suitability of nanoadsorbents for adsorption of Ni(II).
- Nanoadsorbent alumina was found to be quite efficient for the removal of Ni(II) from aqueous solution. It can be used for designing treatment plants for the removal of Ni(II) from water and wastewater.

AUTHOR INFORMATION

Corresponding Author

*E-mail: ysharma.apc@itbhu.ac.in. Phone: +91 5426702865. Fax: +91 542 2368428.

Funding Sources

The authors are thankful to AICTE (Project No. 10313), New Delhi, for providing financial assistance.

REFERENCES

(1) Malakul, P.; Srinivasan, K. R.; Wang, H. Y. Metal adsorption and desorption characteristics of surfactant-modified clay complexes. *Ind. Eng. Chem. Res.* **1998**, *37*, 4296–4301.

(2) Mohan, D.; Singh, K. P. Single and multi-component adsorption of cadmium and zinc using activated carbon derived from bagasse-an agricultural waste. *Water Res.* **2002**, *36*, 2304–2318.

(3) Zafar, M. N.; Abbas, I.; Nadeem, R.; Sheikh, M. A.; Ghauri, M. A. Removal of Nickel onto Alkali Treated Rice Bran. *Water Air Soil Pollut.* **2009**, *197*, 361–370.

(4) Yu, Q.; Kaewsarn, P. Binary adsorption of copper(II)and cadmium(II) from aqueous solutions by biomass of marine alga Durvillaea potatorum. *Sci. Technol.* **1999**, *34* (8), 1595–1605.

(5) Zhao, M.; Duncan, J. R.; Van Hille, R. P. Removal and recovery of zinc from solution and electroplating effluent using Azolla filiculoides. *Water Res.* **1999**, *33* (6), 1516–1522.

(6) Meena, A. K.; Mishra, G. K.; Rai, P. K.; Rajagopal, C.; Nagar, P. N. Removal of heavy metal ions from aqueous solutions using carbon aerogel as an adsorbent. *J. Hazard. Mater.* **2005**, *122*, 161–170.

(7) Rio, M.; Parwate, A. V.; Bhole, A. G. Removal of Cr^{6+} and Ni^{2+} from aqueous solution using bagasse and fly ash. *Waste Manag.* **2002**, *22*, 821–830.

(8) Sharma, Y. C.; Uma; Upadhyay, S. N. Removal of a cationic dye from wastewater by adsorption on activated carbon developed from coconut coir. *Energy Fuels* **2009**, 2986–2988.

(9) Remoudaki, E.; Hatzikioseyian, A.; Tsezos, K.; Tsezos, M. The mechanism of metals precipitation by biologically generated alkalinity in biofilm reactors. *Water Res.* **2003**, *37* (6), 3843–3854.

(10) Sharma, Y. C.; Srivastava, V .; Upadhyay, S. N.; Weng, C. H. Alumina Nanoparticles for the Removal of Ni(II) from aqueous Solutions. *Ind. Eng. Chem. Res.* **2008**, *47*, 8095–8100.

(11) Sharma, Y. C.; Uma; Srivastava, V .; Srivastava, J.; Mahto, M. Reclamation of Cr(VI) rich water and wastewater by wollastonite. *Chem. Eng. J.* **2007**, *127*, 151–156.

(12) Volesky, B.; Holan, Z. R. Biosorption of heavy metals. *Biotechnol. Prog.* **1995**, *11*, 235–250.

(13) Sharma, Y. C.; Srivastava, V .; Singh, V. K .; Kaul, S. N .; Weng, C. H. Nano-adsorbents for the removal of metallic pollutants from water and wastewater. *Environ. Technol.* **2009**, *30*, 583–609.

(14) Dorre, E., Hubner, H., Eds.; *Alumina processing properties and applications*; Springer- Verlag: Berlin, 1984; pp 216−282.

(15) Valente, J. S.; Bokhimi, X.; Toledo, J. A. Synthesis and catalytic properties of nanostructured aluminas obtained by sol-gel method. *Appl. Catal. A: General* **2004**, *264*, 175–81.

(16) Rahmani, A.; Mousavi, H. Z.; Fazli, M. Effect of nanostructure alumina on adsorption of heavy metals. *Desalination* **2010**, *253*, 94–100.

(17) Namdeo, M a.; Bajpai, S. K. Investigation of hexavalent chromium uptake by synthetic magnetite nanoparticles.Electron. *J. Environ. Agric. Food Chem.* **2008**, *7*, 3082–3094.

(18) Nomanbhay, S. M.; Palanisamy, K Removal of heavy metal from industrial wastewater using chitosan coated oil palm shell charcoal. *Electron. J. Biotechnol.* **2005**, *8*, 43–53.

(19) APHA Standard methods for the examination of water and waste water, 14th ed.; APHA, AWWA, 1985.

(20) Ramli, Z.; Chandren, S. Effect of templates on the synthesis of organized mesoporous alumina. *Malaysian J. Anal. Sci.* **2007**, *11*, 110–116.

(21) Vazquez, A.; Lopez, T.; Gomez, R.; Bokhimi, M.; Novarot, O. J. X-Ray Diffraction, FTIR, and NMR characterization of Sol-Gel Alumina Doped with Lanthanum and Cerium. *Solid State Chem.* **1997**, *128*, 161–168.

(22) Robinson, M. D.; Pask, J. A.; Fuerstenau, D. W. Surface charge of alumina and magnesia in aqueous media. *J . Am. Ceram. Soc.* **2006**, *47*, 516–520.

(23) Sag, Y.; Aktay, Y. Mass transfer and equilibrium studies for the sorption of chromium ions onto chitin. *Process. Biochem.* **2000**, *36*, 157–173.

(24) Larous, S.; Meniai, A. H .; Lehocine, M. B. Experimental study of the removal of copper from aqueous solutions by adsorption using sawdust. *Desalination* **2005**, *185*, 483–490.

(25) Ahalya, N.; Kanamadi, R.D .; Ramachandra, T. V. Biosorption of chromium (VI) from aqueous solutions by the husk of Bengal gram (Cicer arientinum). *Electronic. J. Biotechnol.* **2006**, 1–3.

(26) Malkoc, E. Ni(II) removal from aqueous solutions using cone biomass of Thuja orientalis. *J. Hazard. Mater.* **2006**, *137*, 899–908.

(27) Ho, Y. S.; Mckay, G. Pseudo-second order model for sorption processes. *Process Biochem.* **1999**, *34*, 451–465.

(28) Weber, W. J.; Morris, J. C.; Sanit, J. *Eng. Div. Proc. Anal. Soc. Civil Engr. 89 (SA2)* **1963**, *31*, 28.

(29) Knocke, W. R.; Hemphill, L. H. Mercury sorption by waste rubber. *Water Res.* **1981**, *15*, 275–282.

(30) Raghuwanshi, S. P.; Singh, R.; Kaushik, C. P. Kinetic study of methylene blue dye biosorption on baggase. *Appl. Ecol. Environ. Res.* **2004**, *2*, 35–43.

(31) McKay, G.; Otterburn, M. S.; Sweeny, A. G. Surface mass transfer process during colour removal from effluents using silica. *Water Res.* **1981**, *15*, 321–331.

(32) Gupta, G. S.; Prasad, G.; Singh, V. N. Removal of colour from wastewater by sorption for water reuse. *J. Environ. Sci. Health.* **1988**, *A23*, 205–218.

(33) Aksu, Z. Determination of the equilibrium, kinetic and thermodyanamic parameters of the batch adsorption of Ni(II) ions on to Chlorella vulgaris. *Process Biochem.* **2002**, *38*, 89–99.

(34) Sharma, Y. C. *Thermodynamics of removal of cadmium by adsorption on an indegineous clay.* **2008**, *145*, 64–68.

(35) Basha, S.; Murthy, Z. V. P.; Jha, B. Biosorption of hexavalent chromium by chemically modified seaweed, Cystoseira. *Chem. Eng. J.* **2008**, *137*, 480–488.

(36) Ewecharoen, A .; Thiravetyan, P.; Nakbanpote, W. Comparison of nickel adsorption from electroplating rinse water by coir pith and modified coir pith. *Chem. Eng. J.* **2008**, *137*, 181–188.

(37) Dubinin, M. M.; Radushkevich, L. V. Equation of the characteristic curve of activated charcoal. *Proc. Acad. Sci. Phys. Chem. USSR* **1947**, *55*, 331–333.

(38) Wang, X.S.; Qin, Y. Equilibrium sorption isotherms for Cu^{2+} removal on rice bran. *Process Biochem.* **2005**, *40*, 677–680.